




ORIGINAL ARTICLE

Upregulation of S100A10 in metastasized breast cancer stem cells

Hisano Yanagi^{1,2} | Takashi Watanabe¹ | Tatsunori Nishimura³ | Takanori Hayashi¹ |
Seishi Kono⁴ | Hitomi Tsuchida⁵ | Munetsugu Hirata⁶ | Yuko Kijima⁶ |
Shintaro Takao⁴ | Seiji Okada⁷ | Motoshi Suzuki⁸ | Kazuyoshi Imaizumi⁹ |
Kenji Kawada² | Hironobu Minami¹⁰  | Noriko Gotoh³  | Yohei Shimono^{1,5,10} 

¹Department of Biochemistry, Fujita Health University School of Medicine, Toyoake, Japan

²Department of Medical Oncology, Fujita Health University School of Medicine, Toyoake, Japan

³Division of Cancer Cell Biology, Cancer Research Institute, Kanazawa University, Kanazawa, Japan

⁴Division of Breast and Endocrine Surgery, Kobe University Graduate School of Medicine, Kobe, Japan

⁵Division of Molecular and Cellular Biology, Kobe University Graduate School of Medicine, Kobe, Japan

⁶Department of Breast Surgery, Fujita Health University School of Medicine, Toyoake, Japan

⁷Division of Hematopoiesis, Joint Research Center for Human Retrovirus Infection, Kumamoto University, Kumamoto, Japan

⁸Department of Molecular Oncology, Fujita Health University School of Medicine, Toyoake, Japan

⁹Department of Respiratory Medicine, Fujita Health University School of Medicine, Fujita Health University School of Medicine, Toyoake, Japan

¹⁰Division of Medical Oncology/Hematology, Kobe University Graduate School of Medicine, Kobe, Japan

Correspondence

Yohei Shimono, MD, PhD, Department of Biochemistry, Fujita Health University, 1-98 Dengakugakubo, Kutsukake-cho, Toyoake, Aichi 470-1192, Japan.
Email: yshimono@fujita-hu.ac.jp

Funding information

Promotion and Mutual Aid Corporation for Private Schools of Japan; Japan Society for the Promotion of Science, Grant/Award Number: 15K14381 and 18K07231; 19K23900; 20K07600; Princess Takamatsu Cancer Research Fund; Fujita Health University; Cancer Research Institute of Kanazawa University

Abstract

Metastatic progression remains the major cause of death in human breast cancer. Cancer cells with cancer stem cell (CSC) properties drive initiation and growth of metastases at distant sites. We have previously established the breast cancer patient-derived tumor xenograft (PDX) mouse model in which CSC marker CD44⁺ cancer cells formed spontaneous microscopic metastases in the liver. In this PDX mouse, the expression levels of S100A10 and its family proteins were much higher in the CD44⁺ cancer cells metastasized to the liver than those at the primary site. Knockdown of S100A10 in breast cancer cells suppressed and overexpression of S100A10 in breast cancer PDX cells enhanced their invasion abilities and 3D organoid formation capacities in vitro. Mechanistically, S100A10 regulated the matrix metalloproteinase activity and the expression levels of stem cell-related genes. Finally, constitutive knockdown of S100A10 significantly reduced their metastatic ability to the liver in vivo. These findings suggest that S100A10 functions as a metastasis promoter of breast CSCs by conferring both invasion ability and CSC properties in breast cancers.

KEYWORDS

breast cancer, cancer stem cells, metastasis, patient-derived tumor xenograft, S100A10

This is an open access article under the terms of the Creative Commons Attribution-NonCommercial License, which permits use, distribution and reproduction in any medium, provided the original work is properly cited and is not used for commercial purposes.

© 2020 The Authors. *Cancer Science* published by John Wiley & Sons Australia, Ltd on behalf of Japanese Cancer Association.

1 | INTRODUCTION

Breast cancer is now the most frequently diagnosed cancer and the leading global cause of cancer death in women.¹ Despite advances in the diagnosis and treatment of human breast cancer, advanced-stage metastatic breast cancers are difficult to cure.^{2,3} Metastasis involves complex series of cellular and molecular events, characterized by local invasion, intravasation into the blood and lymphatic system, and localization and adaptation to metastatic sites. Distant lymph nodes, bone, lung, liver, and brain are the most common target organs for breast cancer metastasis.⁴ Among them, post-recurrence survival is worst when multiple metastasis is observed in the liver.⁵

Cancer stem cells (CSCs) are a subpopulation of the cells that retain high tumorigenic capacity and, at the same time, are able to sustain the formation of tumors that recreate the cellular diversity of the parent lesions from which they have been originally isolated.⁶ In the specific case of human breast cancers, the subset of cancer cells with CSC properties is enriched among cells defined by the CD44⁺/CD24^{low/neg} phenotype.⁶⁻⁸ We and others have shown that in epithelial malignancies such as breast and colorectal cancers, the self-renewal ability of cancer cells with CSC properties is epigenetically regulated by their expression of microRNAs,⁶ such as miR-200c, miR-142, and miR-221, which suppress the expression of B lymphoma Mo-MLV insertion region 1 homolog (BMI1),^{7,9} adenomatous polyposis coli (APC),¹⁰ and RNA-binding protein Quaking (QKI),¹¹ respectively.

Highly tumorigenic properties of CSCs are associated with metastatic progression, especially at the initial steps of metastases.¹² Indeed, gene expression analysis at the single-cell level has revealed that early-stage metastatic cells possess a distinct stem-like gene expression signature.¹² Modulators of differentiation and stem cell properties regulate metastatic abilities of breast cancer cells. For example, mutation, epigenetic silencing, or reduced expression of luminal differentiation factors in the mammary gland, such as GATA binding protein 3 (GATA3) and E74-like factor 5 (ELF5), and the increased activity of stem cell factors, such as Snail Family Transcriptional Repressor 2 (SNAI2), SRY-Box Transcription Factor 9 (SOX9), Inhibitor of DNA Binding 1 (ID-1), Protein C receptor (PROCR), and Metadherin (MTDH), has been shown to promote metastasis.¹³ We have previously shown that miR-93, which targets Wiskott-Aldrich syndrome protein family (WASF)3, functions as suppressor of CSC properties and metastasis in breast cancer.¹⁴

The S100 protein family is composed of 25 members of small dimeric, EF-hand-type, calcium-binding cytosolic proteins with a molecular weight of 10-12 kDa.^{15,16} Although S100 family members exhibit a high degree of sequence and structural similarity, they are not functionally interchangeable. S100 proteins are involved in multiple intracellular functions, which include: interacting with intracellular receptors or molecule subunits, membrane protein recruitment and transportation, transcriptional regulation, and regulating enzymes, nucleic acids, and DNA repair.¹⁶ Serum amyloid A (SAA) 3, which is induced in premetastatic lungs by S100A8 and S100A9, has a role in the accumulation of myeloid cells and acts as a positive-feedback regulator for chemoattractant

secretion and promotion of metastasis.^{17,18} Phospholipid-binding sites of annexin A2 anchor S100A10 to the cell surface, whereas the carboxyl-terminal lysines of the S100A10 subunits provide the binding sites for tissue plasminogen activator (tPA), plasminogen, and plasmin.¹⁹ The expression level of S100A10 increased by the oncoproteins promyelocytic leukemia/retinoic acid receptor alpha (PML/RAR α) and RAS, and its higher expression is linked to worse outcome in a number of cancer types including breast cancers.²⁰

In this study, we analyzed metastasized CD44⁺ breast cancer cells in breast cancer patient-derived tumor xenograft (PDX) mice to identify the intrinsic factors that were associated with cancer cell metastasis. S100 protein family genes were upregulated in the CD44⁺ PDX cancer cells metastasized to the liver. Among them, S100A10 enhanced invasion ability and organoid-forming capacity of breast cancer cells, both of which are required for metastatic progression. Finally, we found that constitutive knockdown of S100A10 suppressed the metastatic abilities of breast cancer cells *in vivo*.

2 | MATERIALS AND METHODS

2.1 | Flow cytometry

Primary tumor specimens, xenograft tumors, and the liver of the PDX mice were dissociated using collagenase III (Worthington) and analyzed as previously described.¹⁴ Dissociated cells were stained with monoclonal antibodies conjugated to fluorescent dyes. Antibodies used in this study are anti-human CD44-allophycocyanin (APC, clone IM7, 1:20; Biolegend), anti-human leukocyte antigen (HLA) A, B, C-Alexa488 (clone W6/32, 1:20; Biolegend), anti-mouse H-2K^d/H2-D^d-biotin (clone 34-1-2S, 1:40; eBioscience), and anti-mouse Cd45-biotin (clone 30-F11, 1:40; BD Biosciences) antibodies. Dead cells were depleted using 4,6-diamidino-2-phenylindole (DAPI).

2.2 | Gene expression profiling of PDX cells with microarray

Two thousand CD44⁺/HLA⁺ breast cancer PDX cells were sorted from the dissociated xenograft tumors and the liver of the PDX mice. From those cells, total RNA was extracted using RNeasy Mini Kit (Qiagen) according to the manufacturer's instruction. Then, cDNA was synthesized and amplified from total RNA, exploiting the Ovation Pico WTA System V2 (NuGEN). Next, cDNA samples were labeled with cyanine 3-dUTP, exploiting the SureTag DNA Labeling Kit (Agilent Tech.). Finally, cDNAs were subjected to fragmentation and hybridized on the SurePrint G3 Human GE ver3.0 8x60K Microarray (Agilent Tech.) following the manufacturer's instruction. Data were normalized and filtered with three filters using GeneSpring (Agilent Tech.). To compare the gene expression values, we transformed values in normal scale x as follows:

$$\text{value} = \log_2(1 + x).$$

Raw and processed microarray data have been deposited in the GEO repository. The accession number is GSE151191 (GEO reviewer link: <https://www.ncbi.nlm.nih.gov/geo/query/acc.cgi?acc=GSE151191>).

2.3 | Reverse transcription (RT)-semiquantitative real-time PCR (qPCR)

The expression level of S100A10 was analyzed by RT-qPCR as described previously.^{11,14} The following primers were used: S100A10 forward, CAACGGACCACACAAAATGC and reverse, CTGCCTACTTCTTCCCTTCTG; GAPDH forward, AGAAGGCTGGGGC TCATTG and reverse, AGGGGCCATCCACAGTCTTC. Other primers including those used to analyze mRNA expression levels in organoid cells have been described previously.^{14,21} mRNA expression levels were normalized by those of GAPDH. Relative mRNA expression was calculated by using a $\Delta\Delta\text{CT}$ method.

2.4 | Cell lines

MDA-MB-231 and T-47D human breast cancer cells (ATCC catalog: HTB-26 and HTB-133) were obtained from the American Type Culture Collection (ATCC). Cell lines were cultured in Glutamax-containing DMEM (Thermo Fisher Scientific) supplemented with 10% fetal bovine serum (Thermo Fisher Scientific) and penicillin-streptomycin (Thermo Fisher Scientific).

2.5 | Lentivirus production

The sequence of the full-length coding region of the S100A10 mRNA (NM_002966.2 (GenBank)) was amplified by PCR and cloned into the pEIZ-HIV-ZsGreen lentivirus vector (Addgene: #18121).⁷ The shRNA sequences encoding for the S100A10 shRNA constructs (shS100A10) were cloned between the BamHI and EcoRI sites of the miRZIP vector (System Biosciences) and sequenced. The following target sequences were used: shS100A10-1, CCATGATGTTTACATTCACA; shS100A10-5, GACCAGTGTAGAGATGGCAA. A negative control was purchased from System Biosciences. Lentiviruses were produced as previously described.²² The culture supernatant containing lentivirus was collected and concentrated by LentiX concentrator (Clontech) and was resuspended in phosphate-buffered saline. Breast cancer cells constitutively expressing S100A10 shRNA constructs were established by infecting cells with lentivirus constructs at a multiplicity of infection (MOI) of 5 (breast cancer cell line) or of 30 (breast cancer PDX cells). Infected cells were purified based on puromycin resistance (1 $\mu\text{g}/\text{mL}$) or their ZsGreen expression.

2.6 | Gene set enrichment analysis (GSEA)

With respect to relevance to stem cells and invasion, our data were compared to signatures reported by Boquest et al^{23,24} (BOQUEST_STEM_CELL_UP, BOQUEST_STEM_CELL_DN) and Rizki et al²⁵ (RIZKI_TUMOR_INVASIVENESS_2D_DN, RIZKI_TUMOR_INVASIVENESS_2D_UP, RIZKI_TUMOR_INVASIVENESS_3D_DN, RIZKI_TUMOR_INVASIVENESS_3D_UP), respectively. For the metric for ranking genes, \log_2 -Ratio_of_Classes was used. The gene sets with which the comparison with our data showed a false discovery rate (FDR) lower than 0.25 were evaluated as relevant gene sets.

2.7 | Transwell cell invasion assay

Transwell cell invasion assays were performed as described previously,¹⁴ using a 24-well transwell insert with 8 μm pore size (Corning).

2.8 | Gelatin zymography

Gelatin zymography was performed according to the established method.²⁶ Briefly, MDA-MB-231 cells were seeded into a 6-well plate, and from the next day the cells were starved for 48 hours. The culture supernatant was collected and centrifuged at 500 g for 5 min to remove debris, followed by concentration using an Amicon Ultra centrifuge filter (Merck-Sigma). The total amount of protein was determined by Bradford ultra (Expedeon) according to the manufacturer's instruction. The same amount of protein was loaded into SDS-PAGE gel containing gelatin. After electrophoresis, the gel was washed for 30 min twice in washing buffer (2.5% Triton X-100, 5 mmol/L CaCl_2 , 50 mmol/L Tris-HCl [pH 7.5]) and incubated in incubation buffer (1% Triton X-100, 5 mmol/L CaCl_2 , 50 mmol/L Tris-HCl [pH 7.5]) overnight at 37°C. The gel was stained with Coomassie brilliant blue solution to visualize the matrix metalloproteinase (MMP) activity.

2.9 | Organoid assay

Cells constitutively expressing S100A10 shRNA, S100A10, or corresponding control lentivirus constructs were seeded on Matrigel (Corning) in 96-well plates (3 \times 10³ cells/well) and cultured at 37°C with 5% CO₂, as previously described.²⁷ The cells were fixed 8-10 days after seeding with 4% paraformaldehyde for 10 min at room temperature, and then the number of organoids larger than 100 μm (breast cancer PDX cells) or 150 μm (breast cancer cell lines) in diameter was counted under an inverted fluorescent microscope (Axiovert 200, Carl Zeiss) with Plan-Apochromat 20x NA = 0.8. Phase contrast and ZsGreen images were taken by AxioCam under the control of AxioVision. The ZsGreen images were used to measure the diameter.

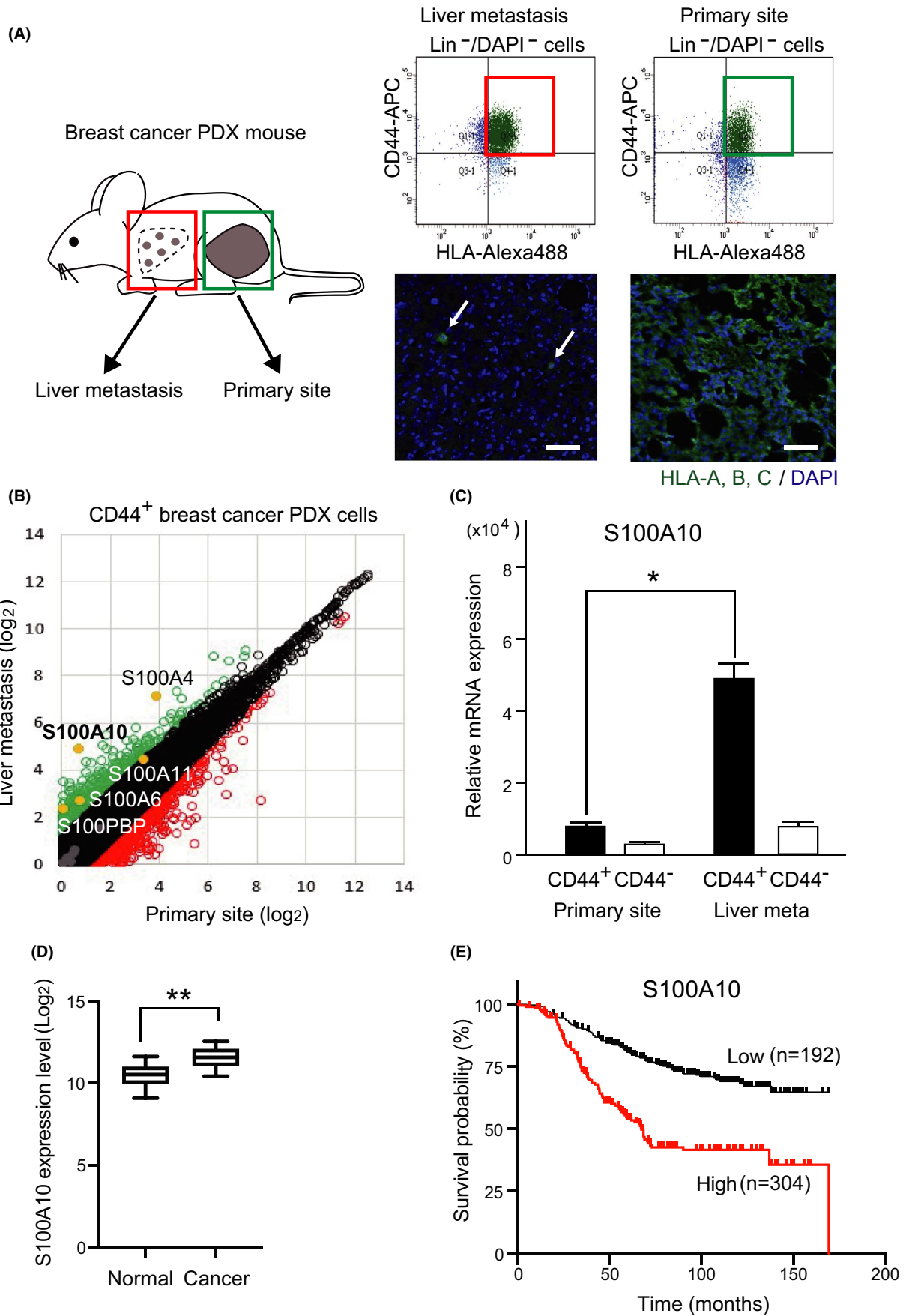


FIGURE 1 Upregulation of S100-family proteins in the CD44⁺ breast cancer patient-derived tumor xenograft (PDX) cells metastasized to the liver. A, Sorting of the cancer stem cell marker CD44⁺ breast cancer cells from the liver and the primary site of breast cancer PDX mouse. Breast cancer PDX-KUB06 cells were transplanted into mouse mammary fat pad. In this PDX mouse model, breast cancer cells spontaneously metastasized to the liver. *Left*: schematic representation of the isolation of PDX cells from the breast cancer PDX mice. *Upper right*: flow cytometry profile of dissociated lin⁻/DAPI⁻ breast cancer PDX cells. CD44⁺ cells within the red or green square gate were sorted. *Lower right*: immunostaining of primary tumor and liver. The tissues were stained with an anti-human HLA A, B, C-Alexa488 antibody for the detection of human breast cancer cells and 4,6-diamidino-2-phenylindole (DAPI). scale bar: 100 μ m. B, Scatter plot of genes expressed in CD44⁺ PDX cells at the primary site and those in the liver. The gene expression levels were plotted using the log₂ of normalized gene expression values. Genes whose expression values were more than two times higher or lower in the CD44⁺ PDX cells metastasized in the liver as compared to those at the primary site are depicted as green and red circles, respectively. Among them, S100 protein family genes whose expression values were more or less than two times higher are colored in yellow and gray, respectively. C, Upregulation of S100A10 in CD44⁺ PDX cells in the liver. Expression levels of S100A10 in the CD44⁺ and CD44⁻ breast cancer cells sorted from the primary tumor or the liver of PDX mice were analyzed using semiquantitative RT-PCR. Data are presented as mean \pm SD, n = 3, *P < 0.05. D, Comparison of S100A10 expression levels in breast cancer and normal tissues from the GENT2 GPL-96 platform (HG-U133A). Box plots display 10th, 25th, 50th, 75th, and 90th percentiles of S100A10 expression levels. **P < 0.0001. E, Relationship between S100A10 expression levels and overall survival rate from the same platform. Association between S100A10 expression levels and survival outcomes was statistically significant (P < 0.0001)

2.10 | Hepatic metastasis model via a splenic injection for competitive transplantation assays

Equal numbers of MDA-MB-231-ZsGreen cells overexpressing S100A10 shRNA (shS100A10-1 ZsGreen) and MDA-MB-231 mCherry competitor were mixed 1:1 and injected into the spleen of NOD/SCID/IL2R γ ^{-/-} (NSG) mice (Charles River) as described previously.¹⁴ After 20 to 30 days following the surgery, the mice were perfused with PBS and the liver was harvested. A part of the liver was fixed for histological examination and the rest of the liver was cut in pieces for dissociation.

2.11 | Statistical analysis

Data are presented as means \pm standard deviation (SD). Comparisons between continuous data normally distributed with equal variance or unequal variances between groups were performed using unpaired two-tailed Student's *t*-tests. Sample sizes, statistical tests, and *P*-values are indicated in the figures or figure legends. All *P*-values were two-sided, and *P*-values < 0.05 or 0.01 were deemed statistically significant. Asterisks denote *P*-value significance.

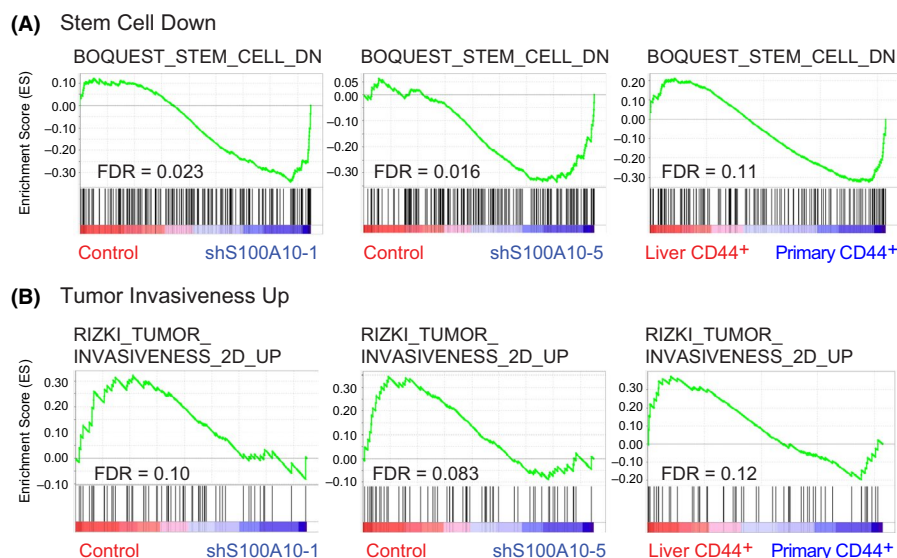


FIGURE 2 Gene set enrichment analysis (GSEA) enrichment score curves. The gene sets for stem cells and tumor invasiveness were less enriched in shS100A10 MDA-MB-231 cells and highly enriched in metastasized cancer stem cells (CSCs) (PDX-KUB06). The y-axis represents the enrichment score (ES) and on the x-axis are genes (vertical black lines) represented in gene sets. The green line connects points of ES and genes. In each graph, probes on the far left (red) correlated with the most upregulated probes in the control MDA-MB-231 cells or CD44⁺ PDX cells metastasized in the liver, and probes on the far right (blue) correlated with the most upregulated probes in shS100A10 MDA-MB-231 cells or CD44⁺ PDX cells in the primary site, respectively. Significance threshold set at FDR < 0.25

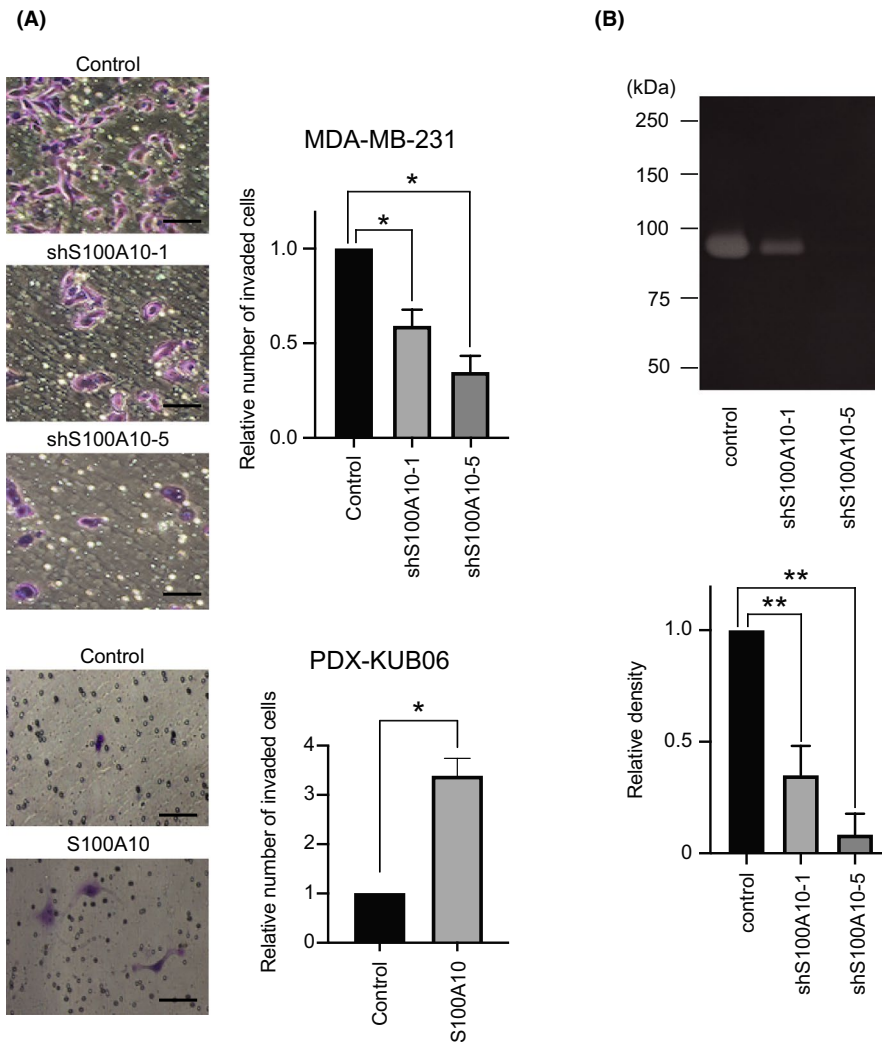


FIGURE 3 The knockdown of S100A10 suppressed the invasion of MDA-MB-231 cells. A, Transwell cell invasion assay was performed using MDA-MB-231 cells constitutively expressing S100A10 shRNA or negative control (upper panels) and PDX-KUB06 cells (lower panels). Cell invasion was measured after 24 h. Representative micrographs and the number of invaded cells in five random fields per membrane are shown. Data are presented as mean \pm SD $n \geq 3$, * $P < 0.05$. B, Gelatin zymography of cells constitutively expressing S100A10 shRNA or negative control. Density of the band at approximately 90 kDa was measured. $n \geq 3$, ** $P < 0.01$

2.12 | Supplementary appendix

Detailed descriptions of the methods including those for the experiments for Supplementary Figures are provided in Appendix S1.

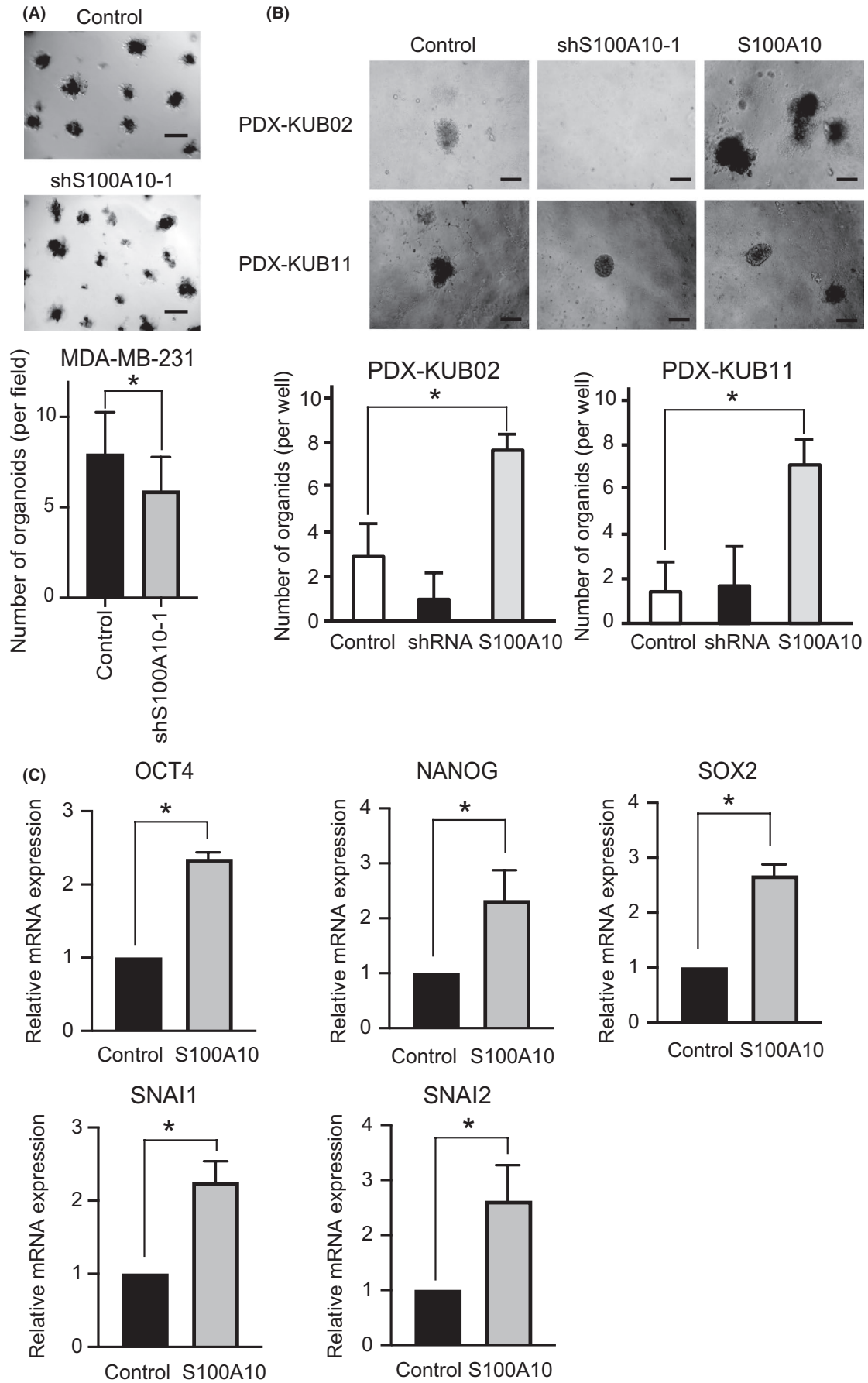
3 | RESULTS

3.1 | Upregulation of S100A10 in the CD44⁺ breast cancer PDX cells metastasized to the liver

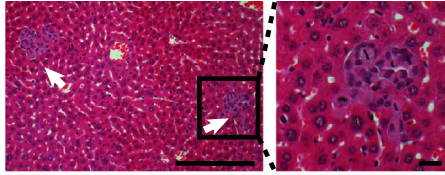
Cancer metastasis is driven by cancer cells with CSC properties which survive multiple steps, including seeding, migration and successful colonization at distant sites.¹² We have previously established the breast cancer PDX mouse model, in which CD44⁺ cancer cells spontaneously metastasized and formed micrometastases at distant sites.^{14,28,29} To

characterize the breast CSCs that are involved in metastatic progression, we analyzed the human breast cancer PDX (KUB06) mouse generated by orthotopic xenotransplantation of luminal-type human breast cancer tissues.²⁸ This PDX mouse is characterized by the formation of micrometastases in the liver when the diameter of tumors at the primary site reached ~2 cm (Figure 1A). In this model, consistent with the previous observation that metastasis is initiated by cancer cells with stem cell program,¹² most of the cells metastasized in the liver were composed of CSC marker CD44⁺ cells (Figure 1A). Comparison of gene expression profiles between the CD44⁺ human breast cancer cells metastasized to the liver ('metastasized CSCs') and those in the primary site ('primary CSCs') revealed that members of the S100 protein family were upregulated in metastasized CSCs compared with primary CSCs (Figure 1B). Given the observed expression patterns, we speculated that these members of the S100 protein family function as enhancers of the metastasis of CD44⁺ PDX cells. Indeed, S100A4, one of the

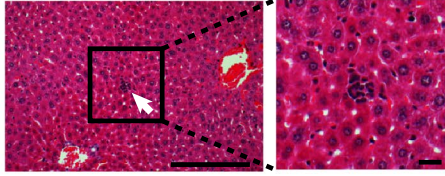
FIGURE 4 S100A10 regulates the 3D organoid formation capacities. A, Constitutive overexpression of S100A10 shRNA reduced the 3D organoid-forming capacity of MDA-MB-231 cells. $n = 3$, * $P < 0.01$, scale bar: 200 μ m. B, Three-dimensional organoid-forming capacity of breast cancer patient-derived tumor xenograft (PDX) cells (KUB02 and 11) infected with lentivirus encoding S100A10 or S100A10 shRNA. $n = 3$, * $P < 0.05$, scale bar: 100 μ m. C, The expression levels of cancer stem cell (CSC) markers. Breast cancer PDX-KUB06 cells constitutively expressing S100A10 or negative control were sphere-cultured for 6 d. The expression levels of CSC markers in PDX cells were measured by semiquantitative PCR. GAPDH was used as a control. * $P < 0.05$



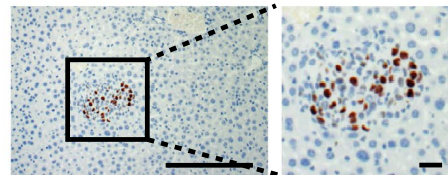
(A) Control



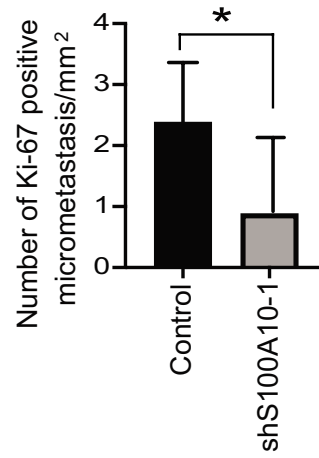
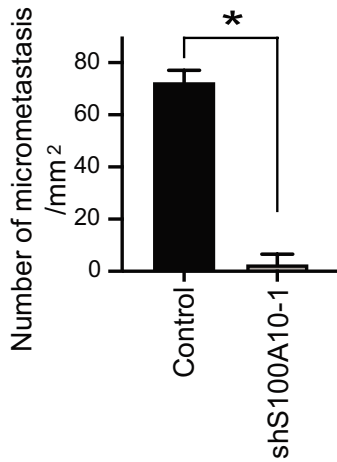
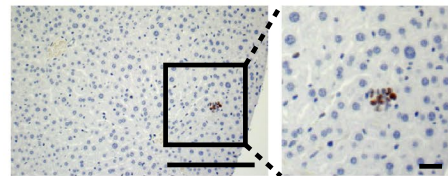
shS100A10-1



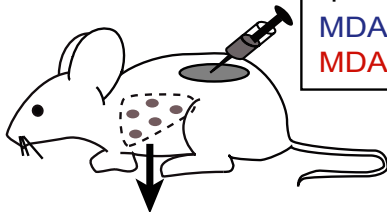
(B) Control



shS100A10-1



(C)



Spleen injection (mixed 1:1)
 MDA-MB-231-ZsGreen cells expressing shS100A10-1
 MDA-MB-231 mCherry competitor (Control)

Analyses of cancer cells metastasized to the liver

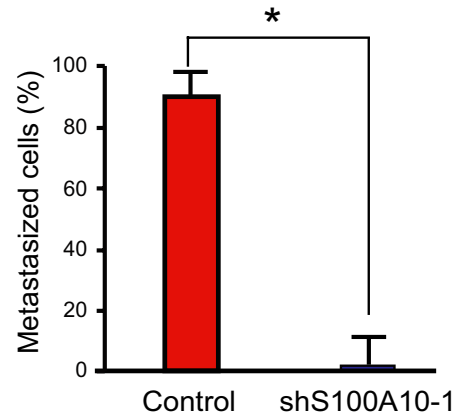
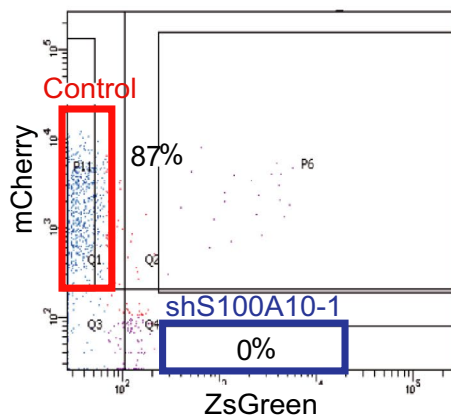


FIGURE 5 Knockdown of S100A10-suppressed liver metastasis in vivo. Spontaneous metastases in the liver were analyzed 8 wk after xenotransplantation. A, Hematoxylin and eosin staining of the liver and number of metastatic foci in the liver. Arrows indicate the representative metastatic foci. B, Ki-67 staining of the liver and number of Ki-67-positive micrometastasis in the liver. Data are presented as mean \pm SD, $n = 6$, $**P < 0.01$, scale bar: 200 μm (low magnification) and 20 μm (high magnification). C, Schematic representation of the splenic injection of tumor cells and competitive transplantation assays. For the competitive transplantation assay, MDA-MB-231-ZsGreen cells overexpressing shS100A10-1 and MDA-MB-231 mCherry competitor (mixed 1:1) were transplanted into the spleen of immunodeficient NSG mice. The liver was perfused and dissociated 3 wk after the transplantation. Percentage of donor chimerism of the cancer cells metastasized in the liver was analyzed using a flow cytometry. Data are presented as mean \pm SD, $n = 3$, $*P < 0.05$

highly upregulated S100 protein family members in the metastasized CSCs, promotes metastasis, and its higher expression is associated with poorer patient outcome.³⁰ In this study, we focused on S100A10, which was one of the most highly upregulated S100 protein in metastasized CSCs compared with primary CSCs (Figure 1B). We then analyzed the expression levels of S100A10 in CD44⁺ and CD44⁻ cancer cells at the primary site and in the liver. Upregulation of S100A10 mRNA in metastasized cancer cells was highly specific to CD44⁺ PDX cells metastasized in the liver, and its expression level was significantly lower in CD44⁻ PDX cells metastasized in the liver and both CD44⁺ and CD44⁻ PDX cells at the primary site (Figure 1C). Analyses of database revealed that the expression level of S100A10 was significantly higher in cancer tissue than in normal tissue, and its higher expression was associated with poorer patient outcome (Figure 1D and E).

3.2 | S100A10 knockdown suppressed cell invasion abilities

Because S100A10 was upregulated in the CD44⁺ PDX cells successfully metastasized to the liver, first we evaluated the roles of S100A10 in cellular functions, such as cell proliferation, death, migration, and invasion of breast cancer cells. Breast cancer MDA-MB-231 cells were infected with lentivirus encoding shRNA sequences against S100A10 (Figure S1). GSEA revealed that S100A10 may regulate stem cell phenotype and tumor invasiveness (Figure 2). Constitutive knockdown of S100A10 did not significantly affect cell proliferation, cell cycle progression, apoptosis, and migration of MDA-MB-231 cells (Figure S2 and S3). In contrast, in transwell cell invasion assays in which the upper surface of transwell inserts was precoated with Matrigel, constitutive knockdown of S100A10 using shS100A10-1 or -5 significantly reduced the number of MDA-MB-231 breast cancer cells invaded by 40% and 60%, respectively (Figure 3A). Cell surface S100A10 binds to annexin A2 and cleaves and activates plasminogen, which then activates MMPs, such as MMP-3, -9, -12, and -13.³¹ The results of gelatin zymography showed that knockdown of S100A10 significantly reduced the activity of MMP9 (gelatinase B) in MDA-MB-231 cells (Figure 3B). Finally, to confirm that the effects of S100A10 on breast cancer cells were observed irrespective of hormone receptor status, we infected shS100A10 to luminal-type breast cancer T-47D cells, and overexpressed S100A10 in luminal-type breast cancer PDX-KUB06 cells which weakly express S100A10. Knockdown of S100A10 in T-47D cells reduced and overexpression of S100A10 in PDX-KUB06 cells enhanced the cell invasion abilities without affecting their cell cycle progression

and apoptosis (Figure 3A, Figures S4 and S5). These results suggest that S100A10 functions as a regulator of cell invasion in both hormone receptor positive and negative breast cancer cells and PDX cells.

3.3 | S100A10 enhanced the organoid-forming capacity of PDX cells

Acquisition and enhancement of CSC properties upregulate metastatic potential of cancer cells. To understand whether S100A10 had a direct mechanistic role in enhancing CSC properties, we tested whether S100A10 was able to affect the three-dimensional (3D) organoid-forming capacity of breast cancer cells. Organoid culture is a 3D culture method that enables ex vivo analysis of stem cell behavior and differentiation.²⁷ Infection of MDA-MB-231 cells with a lentivirus encoding for shS100A10-1 significantly reduced their capacity to grow as 3D organoids (Figure 4A). We then analyzed the effect of S100A10 on the 3D organoid-forming capacity of luminal-type breast cancer PDX cells. Breast cancer PDX cells isolated from the primary site of PDX mice were infected with a lentivirus encoding for S100A10. Constitutive overexpression of S100A10 significantly increased their capacity to grow as 3D organoids and enhanced the expression of stem cell-related genes, such as POU Class 5 Homeobox 1 (OCT4, POU5F1), SOX2, Nanog Homeobox (NANOG), SNAI1/2 (Figure 4B and C). In contrast, constitutive knockdown of S100A10 did not significantly reduce the number of 3D organoids formed by breast cancer PDX cells (Figure 4B), possibly because of low expression levels of S100A10 in the CD44⁺ PDX cells.

3.4 | S100A10 promotes the metastatic capacity of breast cancer cells in vivo

Because S100A10 is a regulator of cell invasion and 3D organoid-forming capacities in vitro, we tested whether constitutive knockdown of S100A10 was able to suppress metastasis of breast cancer cells in immunodeficient NSG mice. MDA-MB-231 cells overexpressing shS100A10-1 or control MDA-MB-231 cells were orthotopically transplanted at the mammary fat pad region of NSG mice. Consistent with in vitro proliferation and apoptosis assays (Figure S2), constitutive knockdown of S100A10 did not affect tumor growth at the primary sites in vivo (Figure S6). However, in vivo metastatic capacity was significantly reduced in MDA-MB-231 cells constitutively overexpressing shS100A10-1 (Figure 5A). Micrometastases in the liver of the mice transplanted with shS100A10-1 cells were smaller in

number and size, and the number of Ki-67 positive micrometastases was significantly smaller than that in the mouse transplanted with control cells (Figure 5A and B). Finally, we performed a competitive transplantation assay which is able to recapitulate the latter half of the metastatic cascades (ie, interaction with blood cells, extravasation, and/or colonization)³² to further confirm that S100A10 affects metastatic capacities of breast cancer cells *in vivo*. When MDA-MB-231-ZsGreen cells constitutively overexpressing shS100A10-1 and MDA-MB-231-mCherry competitor (mixed 1:1) were transplanted into the spleen of immunodeficient NSG mice, the percentage of MDA-MB-231 mCherry competitor cells was significantly higher than that of shS100A10-1 ZsGreen cells among the cancer cells successfully colonized to the liver (Figure 5C). These results suggest that breast cancer cells with constitutive reduction of S100A10 had a significant competitive disadvantage in the liver metastasis.

4 | DISCUSSION

Upregulation of S100-family protein expression is observed in many human cancers, including breast, lung, bladder, and gastric cancers.³³ For example, S100 proteins, such as S100A4, S100A7, S100A8, S100A9, and S100A11, secreted from cancer cells and stromal cells actively contribute to tumorigenic processes such as cell proliferation, metastasis, angiogenesis, and immune evasion.³³⁻³⁷ S100A10 is a unique member of the S100 protein family because it lacks a functional EF domain that mediates calcium ion-dependent protein-protein interactions. In this study, we showed that upregulation of both invasion ability and CSC properties are part of the mechanisms by which S100A10 confers metastatic potential to breast cancer cells and PDX cells. The fact that upregulation of S100A10 was characteristically observed in the CD44⁺ breast cancer cells but not in CD44⁻ breast cancer cells among the metastasized cells in the liver (Figure 1C) further supports a notion that S100A10 has specific roles in the regulation of the metastasis of breast cancer CSCs *in vivo*. Although S100A10 promotes multiple oncogenic properties including proliferation, invasion, and migration especially in ovarian cancers,^{38,39} the effect of S100A10 on proliferation and migration was not evident in breast cancer cells and PDX cells, suggesting that the effect of S100A10 on oncogenic properties is cell type-dependent (Figure S2-S6).

The interaction of S100A10 with annexin A2 and plasmin activates various signaling molecules highly associated with CSC properties and/or cell invasion, including nuclear factor- κ B (NF- κ B), signal transducer and activator of transcription 3 (STAT3), and interleukin-6 signaling pathways.^{40,41} In addition, intracellular S100A10 binds to many binding partners, including annexin A2, protein kinase

PCTAIRE-1, phospholipase A2, and Bcl-2-associated death promoter (BAD).⁴¹ We found that stem cell-related genes such as OCT4, SOX2, and NANOG were upregulated by S100A10 in PDX-derived organoids, and the pathways related to stem cell characters and tumor invasiveness are enriched by S100A10 overexpression (Figures 2 and 4C). Together with our previous report that miR-93 functions as a

metastasis suppressor by targeting WASF3, a regulator of both CSC properties and cell invasion,¹⁴ our findings suggest that S100A10 is among the molecules that promote metastasis of breast cancer CSCs especially at the initial stage of metastasis.

On the other hand, the carboxyl-terminal lysines of S100A10 bind to tPA and plasminogen, which stimulate plasmin production.⁴² Active plasmin degrades matrix proteins and then activates other proteases, including MMP-2 and MMP-9 gelatinases that play a role in the invasion and metastasis of cancer through the destruction of the basal membrane and extracellular matrix. Endothelial cells from S100A10-null mice demonstrated a 40% reduction in plasminogen binding and plasmin generation *in vitro*.¹⁹ In human macrophage, loss of S100A10 expression results in a decrease in MMP-9 activation.⁴³ Taken together, these data suggest that MMP-9 activation is one of the mechanisms involved in the upregulation of invasion abilities (Figure 3). Indeed, higher expression of MMP-9 is significantly associated with a higher incidence of metastasis and relapse in breast cancer.^{44,45}

Emerging *in vivo* evidence indicates that the biology of most S100 proteins is complex and multifactorial.³³ Considering the roles of tumor-associated macrophages (TAMs) in CSC properties, growth, and metastasis of breast cancer cells,^{46,47} it is noteworthy to point out that S100A10 is a major mediator of macrophage recruitment in response to an inflammatory stimulus *in vivo*.⁴³ Together, these data suggest the presence of multiple mechanisms by which S100A10 serves as an enhancer of CSC properties especially in the metastasis of breast cancers.

ACKNOWLEDGEMENTS

We thank Drs. Masao Maeda (Fujita Health University, Japan), Atsushi Enomoto (Nagoya University, Japan), Hidemasa Goto (Mie University, Japan), Miki Nishio, Junko Mukohyama, Jyunji Otani, and Tomohiko Maehama (Kobe University, Japan) for their superior supports and discussions. This work was supported by grants from (1) the Japan Society for the Promotion of Science (JSPS KAKENHI) (15K14381, 18K07231, and Japan-Belgium Research Cooperative Program to YS; 19K23900 and 20K07600 to TW), (2) the Princess Takamatsu Cancer Research Fund (to YS), (3) the Fujita Health University (to YS), (4) the Cancer Research Institute of Kanazawa University (to YS), and (5) the Promotion and Mutual Aid Corporation for Private Schools of Japan (to YS).

CONFLICT OF INTEREST

The authors declare no competing interests.

ETHICAL APPROVAL

Human primary breast cancers were obtained from patients admitted to the Kobe University Hospital and the Fujita Health University Hospital. The research was preapproved by Kobe University's Institutional Review Board (permission number: 1299 and 1481) and Fujita Health University's Institutional Review Board (permission number: HM19-105) and was conducted in accordance with recognized ethical guidelines. All patients included in the study provided written informed consent. Animal experiments were performed with the approval of Kobe University's

Animal Care and Use Committee (permission number: P100905 and P150802) and Fujita Health University's Animal Care and Use Committee (permission number: AP19062) and carried out according to the Animal Experiment Regulations of Kobe and Fujita Health Universities.

ORCID

Hironobu Minami  <https://orcid.org/0000-0001-8630-9145>

Noriko Gotoh  <https://orcid.org/0000-0003-3733-260X>

Yohei Shimono  <https://orcid.org/0000-0002-6256-4704>

REFERENCES

- Bray F, Ferlay J, Soerjomataram I, Siegel RL, Torre LA, Jemal A. Global cancer statistics 2018: GLOBOCAN estimates of incidence and mortality worldwide for 36 cancers in 185 countries. *CA Cancer J Clin*. 2018;68:394-424.
- Redig AJ, McAllister SS. Breast cancer as a systemic disease: a view of metastasis. *J Intern Med*. 2013;274:113-126.
- O'Shaughnessy J. Extending survival with chemotherapy in metastatic breast cancer. *Oncologist*. 2005;10(Suppl 3):20-29.
- Jin X, Mu P. Targeting Breast Cancer Metastasis. *Breast Cancer (Auckl)*. 2015;9:23-34.
- Kimbung S, Johansson I, Danielsson A, et al. Transcriptional Profiling of Breast Cancer Metastases Identifies Liver Metastasis-Selective Genes Associated with Adverse Outcome in Luminal A Primary Breast Cancer. *Clin Cancer Res*. 2016;22:146-157.
- Shimono Y, Mukohyama J, Nakamura S, Minami H. MicroRNA Regulation of Human Breast Cancer Stem Cells. *J Clin Med*. 2015;5(1):2.
- Shimono Y, Zabala M, Cho RW, et al. Downregulation of miRNA-200c links breast cancer stem cells with normal stem cells. *Cell*. 2009;138:592-603.
- Al-Hajj M, Wicha MS, Benito-Hernandez A, Morrison SJ, Clarke MF. Prospective identification of tumorigenic breast cancer cells. *Proc Natl Acad Sci U S A*. 2003;100:3983-3988.
- Wellner U, Schubert J, Burk UC, et al. The EMT-activator ZEB1 promotes tumorigenicity by repressing stemness-inhibiting microRNAs. *Nat Cell Biol*. 2009;11:1487-1495.
- Isobe T, Hisamori S, Hogan DJ, et al. miR-142 regulates the tumorigenicity of human breast cancer stem cells through the canonical WNT signaling pathway. *Elife*. 2014;3.
- Mukohyama J, Isobe T, Hu Q, et al. miR-221 Targets QKI to Enhance the Tumorigenic Capacity of Human Colorectal Cancer Stem Cells. *Cancer Res*. 2019;79:5151-5158.
- Lawson DA, Bhakta NR, Kessenbrock K, et al. Single-cell analysis reveals a stem-cell program in human metastatic breast cancer cells. *Nature*. 2015;526:131-135.
- Celia-Terrassa T, Kang Y. Distinctive properties of metastasis-initiating cells. *Genes Dev*. 2016;30:892-908.
- Shibuya N, Kakeji Y, Shimono Y. miR-93 targets WASF3 and functions as a metastasis suppressor in breast cancer. *Cancer Sci*. 2020.
- Chen H, Xu C, Jin Q, Liu Z. S100 protein family in human cancer. *Am J Cancer Res*. 2014;4:89-115.
- Xia C, Braunstein Z, Toomey AC, Zhong J, Rao X. S100 Proteins as an important regulator of macrophage inflammation. *Front Immunol*. 2017;8:1908.
- Hiratsuka S, Watanabe A, Aburatani H, Maru Y. Tumour-mediated upregulation of chemoattractants and recruitment of myeloid cells predetermines lung metastasis. *Nat Cell Biol*. 2006;8:1369-1375.
- Hiratsuka S, Watanabe A, Sakurai Y, et al. The S100A8-serum amyloid A3-TLR4 paracrine cascade establishes a pre-metastatic phase. *Nat Cell Biol*. 2008;10:1349-1355.
- Surette AP, Madureira PA, Phipps KD, Miller VA, Svenningsson P, Waisman DM. Regulation of fibrinolysis by S100A10 in vivo. *Blood*. 2011;118:3172-3181.
- Saiki Y, Horii A. Multiple functions of S100A10, an important cancer promoter. *Pathol Int*. 2019;69:629-636.
- Goto H, Shimono Y, Funakoshi Y, et al. Adipose-derived stem cells enhance human breast cancer growth and cancer stem cell-like properties through adipisin. *Oncogene*. 2019;38:767-779.
- Tiscornia G, Singer O, Verma IM. Production and purification of lentiviral vectors. *Nat Protoc*. 2006;1:241-245.
- Subramanian A, Tamayo P, Mootha VK, et al. Gene set enrichment analysis: a knowledge-based approach for interpreting genome-wide expression profiles. *Proc Natl Acad Sci U S A*. 2005;102:15545-15550.
- Boquest AC, Shahdadfar A, Fronsdal K, et al. Isolation and transcription profiling of purified uncultured human stromal stem cells: alteration of gene expression after in vitro cell culture. *Mol Biol Cell*. 2005;16:1131-1141.
- Rizki A, Weaver VM, Lee SY, et al. A human breast cell model of preinvasive to invasive transition. *Cancer Res*. 2008;68:1378-1387.
- Toth M, Fridman R. Assessment of Gelatinases (MMP-2 and MMP-9) by Gelatin Zymography. *Methods Mol Med*. 2001;57:163-174.
- Shimono Y, Mukohyama J, Isobe T, Johnston DM, Dalerba P, Suzuki A. Organoid culture of human cancer stem cells. *Methods Mol Biol*. 2019;1576:23-31.
- Nobutani K, Shimono Y, Mizutani K, et al. Downregulation of CXCR4 in Metastasized Breast Cancer Cells and Implication in Their Dormancy. *PLoS One*. 2015;10:e0130032.
- Liu H, Patel MR, Prescher JA, et al. Cancer stem cells from human breast tumors are involved in spontaneous metastases in orthotopic mouse models. *Proc Natl Acad Sci U S A*. 2010;107:18115-18120.
- Boye K, Maelandsmo GM. S100A4 and metastasis: a small actor playing many roles. *Am J Pathol*. 2010;176:528-535.
- Lijnen HR. Plasmin and matrix metalloproteinases in vascular remodeling. *Thromb Haemost*. 2001;86:324-333.
- Lambert AW, Pattabiraman DR, Weinberg RA. Emerging biological principles of metastasis. *Cell*. 2017;168:670-691.
- Bresnick AR, Weber DJ, Zimmer DB. S100 proteins in cancer. *Nat Rev Cancer*. 2015;15:96-109.
- Tomonobu N, Kinoshita R, Sakaguchi M. S100 soil sensor receptors and molecular targeting therapy against them in cancer metastasis. *Transl Oncol*. 2020;13:100753.
- Takamatsu H, Yamamoto KI, Tomonobu N, et al. Extracellular S100A11 plays a critical role in spread of the fibroblast population in pancreatic cancers. *Oncol Res*. 2019;27:713-727.
- Chen Y, Sumardika IW, Tomonobu N, et al. Critical role of the MCAM-ETV4 axis triggered by extracellular S100A8/A9 in breast cancer aggressiveness. *Neoplasia*. 2019;21:627-640.
- Ren D, Zhu X, Kong R, et al. Targeting Brain-Adaptive Cancer Stem Cells Prohibits Brain Metastatic Colonization of Triple-Negative Breast Cancer. *Cancer Res*. 2018;78:2052-2064.
- Tantyo NA, Karyadi AS, Rasman SZ, Salim MRG, Devina A, Sumarmo A. The prognostic value of S100A10 expression in cancer. *Oncol Lett*. 2019;17:1417-1424.
- Wang L, Yan W, Li X, et al. S100A10 silencing suppresses proliferation, migration and invasion of ovarian cancer cells and enhances sensitivity to carboplatin. *J Ovarian Res*. 2019;12:113.
- Jost M, Gerke V. Mapping of a regulatory important site for protein kinase C phosphorylation in the N-terminal domain of annexin II. *Biochim Biophys Acta*. 1996;1313:283-289.
- Madureira PA, O'Connell PA, Surette AP, Miller VA, Waisman DM. The biochemistry and regulation of S100A10: a multifunctional plasminogen receptor involved in oncogenesis. *J Biomed Biotechnol*. 2012;2012:353687.

42. Kwon M, MacLeod TJ, Zhang Y, Waisman DM. S100A10, annexin A2, and annexin a2 heterotetramer as candidate plasminogen receptors. *Front Biosci*. 2005;10:300-325.
43. O'Connell PA, Surette AP, Liwski RS, Svenningsson P, Waisman DM. S100A10 regulates plasminogen-dependent macrophage invasion. *Blood*. 2010;116:1136-1146.
44. Sullu Y, Demirag GG, Yildirim A, Karagoz F, Kandemir B. Matrix metalloproteinase-2 (MMP-2) and MMP-9 expression in invasive ductal carcinoma of the breast. *Pathol Res Pract*. 2011;207:747-753.
45. Yousef EM, Tahir MR, St-Pierre Y, Gaboury LA. MMP-9 expression varies according to molecular subtypes of breast cancer. *BMC Cancer*. 2014;14:609.
46. Gyorki DE, Asselin-Labat ML, van Rooijen N, Lindeman GJ, Visvader JE. Resident macrophages influence stem cell activity in the mammary gland. *Breast Cancer Res*. 2009;11:R62.
47. Jinushi M, Chiba S, Yoshiyama H, et al. Tumor-associated macrophages regulate tumorigenicity and anticancer drug

responses of cancer stem/initiating cells. *Proc Natl Acad Sci U S A*. 2011;108:12425-12430.

SUPPORTING INFORMATION

Additional supporting information may be found online in the Supporting Information section.

How to cite this article: Yanagi H, Watanabe T, Nishimura T, et al. Upregulation of S100A10 in metastasized breast cancer stem cells. *Cancer Sci* 2020;111:4359–4370. <https://doi.org/10.1111/cas.14659>